2 RESULTS AND DISCUSSION

2.1 THE NUCLEAR ENVELOPE PROTEOME

To identify novel inner nuclear membrane proteins, the proteome of the nuclear envelope was characterized, using a combination of subcellular fractionation, 16-BAC-/SDS-polyacrylamide gel electrophoresis and MALDI mass spectrometry (subcellular proteomics). The 'candidates' were characterized using tools of bioinformatics and their localization to the nuclear membrane was confirmed by immunofluorescence on cells that transiently expressed epitope-tagged versions of these proteins. The first part – the subcellular proteomics – was carried out by Mathias Dreger and will be presented here as a short summary that is necessary for a better understanding of the following work.

2.1.1 Fractionation of nuclear envelopes and the protein content of the fractions

The initial NE preparation contains the nuclear membranes, nuclear pore complexes, the nuclear lamina, lamina-interacting nuclear matrix and associated proteins and represents 6 % of the total nuclear protein. For the separation of NE proteins, the 16-BAC-/SDS-PAGE system was used, because of its ability to represent integral membrane proteins.

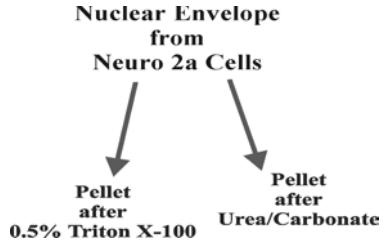

Fig. 2-1 Fractionation of the nuclear envelope – scheme. The fractionation of the nuclear envelope was designed to be a one-step procedure. A sequential extraction with first detergent and then chaotrope would lead to the formation of aggregates, as was observed in previous experiments.

The initial NE preparation was fractionated with either TX-100 or urea/carbonate (fig. 2-1) to reduce the sample complexity since the 16-BAC-/SDS-PAGE gels result in a rather limited resolution of proteins. Additionally, while it is technically impossible to separate INM from ONM and ER, the fractionation allowed the preparation of subsets of NE proteins derived from distinct NE subcompartments.

The fractions were characterized according to the distribution of specific marker proteins. Lamin B1 was chosen as a marker protein for the nuclear lamina and the transmembrane chaperone calnexin as a marker for the ONM/ER. The INM was traced using LAP 2β as a marker protein. LAP 2β is an integral membrane protein of the INM, interacts with the nuclear lamina and chromatin and is resistant to limited extraction by TX-100. The comparison of the protein patterns of the different pellet fractions revealed striking differences in the distribution of the marker proteins (fig. 2-2): LAP 2β was observed as a major protein spot in both TX-100 and urea/carbonate fractions, calnexin was absent from the TX-100 extracted NE preparation and the amount of lamin B1 was significantly reduced in urea/carbonate washed NE.

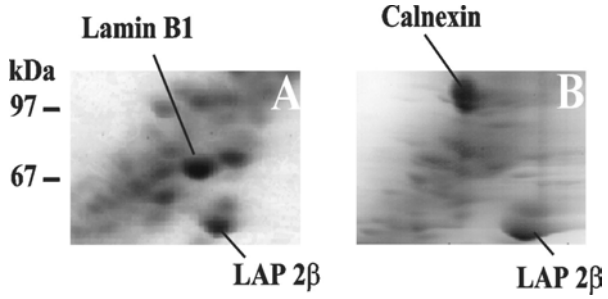

Fig. 2-2 Sections of BAC/SDS-PAGE where the marker proteins were found. LAP 2β and lamin B1 were found in the TX-100 extracted nuclear envelopes (A), calnexin and LAP 2β were present in the carbonate/urea washed nuclear envelopes (B). The image was kindly provided by M. Dreger.

This indicates that the ONM/ER-membrane was removed by TX-100 treatment, that lamina and lamina-interacting nuclear matrix and associated proteins are absent in the chaotrope-resistant fraction and that INM proteins are present in both fractions. Consistent with the distribution of the marker proteins, characteristic differences between the entire protein ensembles were observed when comparing the TX-100 and the chaotrope resistant fraction (fig. 2-3).

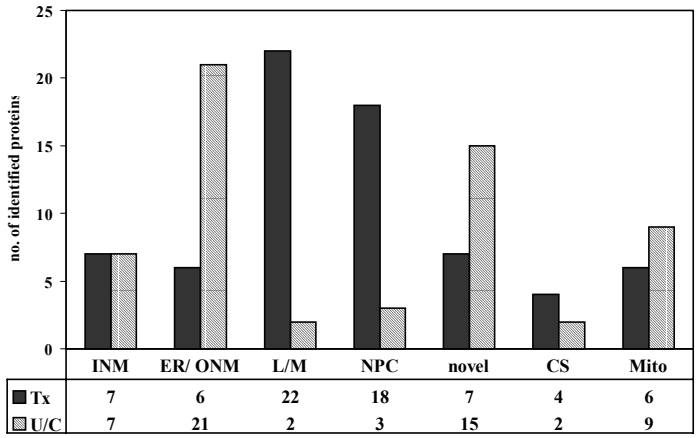

Fig. 2-3 Selected proteins detected in the TX-100 resistant nuclear envelope fraction (Tx) and in the chaotrope resistant fraction (U/C) grouped according to their subcellular localization. INM, inner nuclear membrane, ER/ONM, endoplasmic reticulum/outer nuclear membrane, L/M, nuclear lamina and attached protein scaffold, NPC, nuclear pore complex, CS, cytoskeleton, Mito, mitochondria. Note the differences in the distribution of ER/ONM protein, L/M proteins and NPC proteins.

In total, 148 different proteins were identified. Nineteen proteins were gene products corresponding to ESTs or full-length open reading frames without any functional and subcellular localization annotation and were identified at the protein level for the first time. The most striking differences were found in the distribution of nucleoporins, the proteins of the nuclear lamina and the attached scaffold, and the ER/ONM proteins. The distribution of INM proteins differed only in the abundance of emerin (see below). The presence of mitochondrial proteins in both fractions is most probably due to a minor contamination of the NE preparation. It is difficult to eliminate or reduce this contamination, because of the morphological characteristics of the cell system used (in N2a cells, mitochondria seem to be present in the nuclear invaginations), and the enrichment of mitochondrial proteins by extraction with urea.

For complete lists of the identified proteins, annotated gel pictures and details of the identification procedure see Dreger et al., 2001.

2.1.2 Discovery of two novel proteins of the inner nuclear membrane

Both fractions contained most of the known integral membrane proteins of the INM, namely nurim, lamin B receptor, transmembrane LAP 2 splice variants β, γ, δ, and ε, and MAN-1. Additionaly, emerin was found in the urea/carbonate-resistant fraction. The integral membrane proteins of the INM were the only transmembrane proteins found in both fractions. Therefore, we assumed that every hitherto unknown transmembrane protein which is present in both fractions, should be a novel INM protein. The term 'novel protein' refers to proteins, which have not yet been identified at the protein level, and are merely known as cDNA entries in the data bases. Two such proteins were found (fig. 2-4): the murine homologue of KIAA0810 encoded by the RIKEN cDNA clone with the sequence ID 5730434D03 (FANTOM database at http//www.gsc.riken.go.jp/e/FANTOM) was identified at an apparent molecular mass of ~100 kDa and a putative integral membrane protein of 45 kDa (PID 12836214). The proteins were named mKIAA0810 (murine KIAA0810) and LUMA (because at this stage nothing was known about the function of LUMA, the protein was named after its discoverers: Luiza and Mathias).

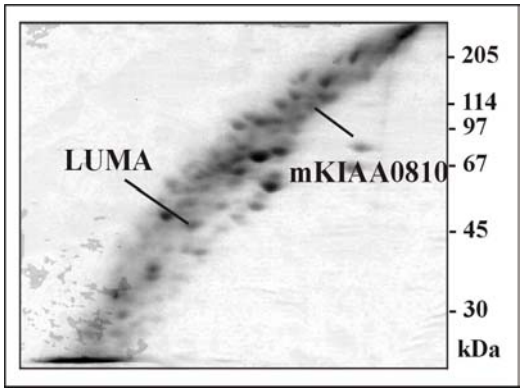

Fig. 2-4 Position of LUMA and mKIAA0810 on a typical BAC/SDS-PAGE. mKIAA0810 migrates at an apparent Mw of ~100kDa, LUMA at 45kDa. The image was kindly provided by M. Dreger.

2.1.3 Localization of KIAA0810 and LUMA in COS-7 cells

To prove that mKIAA0810 and LUMA are indeed proteins of the INM, the subcellular localization of the two proteins was assessed by indirect immunofluorescence on transiently transfected cells overexpressing these two proteins. The DNA corresponding to the coding sequence of human KIAA0810 was amplified by PCR from its cDNA clone, yielding a

2500 bp fragment. The PCR product was cloned into pcDNA3.1/V5-His - an eukaryotic expression vector, which allows the expression of proteins carrying a C-terminal His_6- and V5-tag. The DNA corresponding to the coding sequence of murine LUMA was amplified from N2a cell cDNA, yielding a 1200 bp fragment which was also cloned into the pcDNA3.1/V5-His vector. The COS-7 cells were transfected with these plasmids and the distribution of the proteins was examined by immunofluorescence microscopy using the anti-V5 antibody. Indirect immunofluorescence detected by confocal laser scanning microscopy with KIAA0810-transfected (fig. 2-5 A) and LUMA-transfected COS-7 cells (fig. 2-5 B) revealed in both cases a rim-like fluorescence patterns around the nucleus typical for integral membrane proteins of the INM.

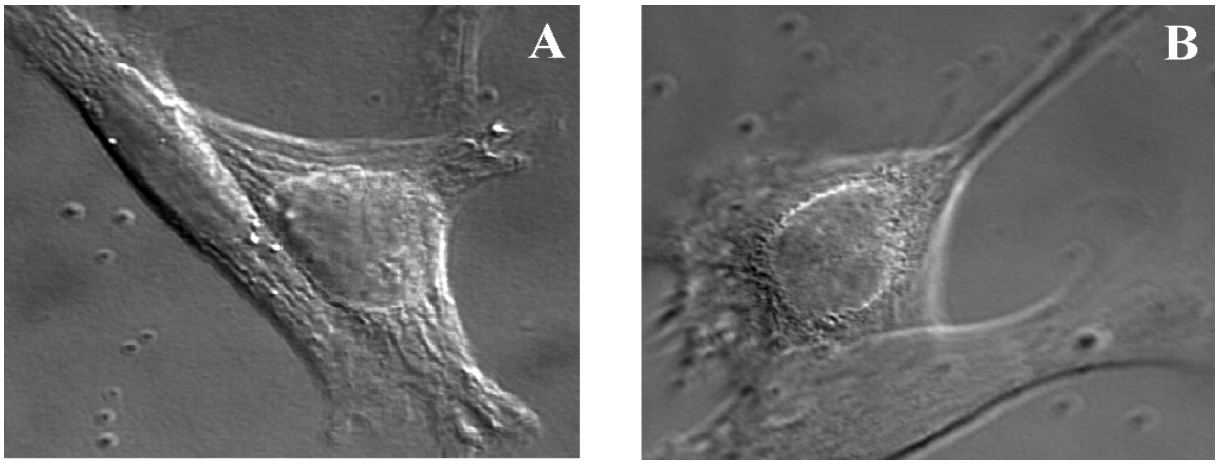

Fig. 2-5 Overexpression of KIAA0810 and LUMA in COS-7 cells. Overexpressed KIAA0810 and LUMA give rise to a rim-like staining around the nucleus as visualized by indirect immunofluorescence: COS-7 cells were transfected with plasmids for the expression of V5-tagged KIAA0810 (A) and LUMA (B). Immunofluorescence studies were carried out with permeabilized cells grown on glass cover slips, as described under Methods. Fluorescence images were obtained with a confocal laser scanning microscope. The microscopy was performed by Torsten Schöneberg.

These two proteins are the first of the novel proteins for which we could demonstrate a localization in the INM. 148 proteins were identified in total, 19 of them were previously unknown, two of these turned out to be novel INM proteins. About 12 INM proteins were known before this study. By adding two more, the list of INM proteins is far from being complete. Many more INM proteins can be expected to be there. The discovery of LUMA and mKIAA0810 was possible, because both proteins are fairly abundant. Other less abundant

proteins may remain undetected because of the limitations of the applied techniques. The BAC/SDS-PAGE is capable of separating integral membrane proteins, but with a rather limited resolution. This often results in the presence of more than one protein in one spot, which in turn gives rise to a very heterogenous peptide mixture after *in-gel* digestion. This situation is a challenge for MALDI MS, since the peptides compete for the energy of the laser. Some of the peptides are better extracted by the laser pulse, are ionized more easily and are thus more likely to be detected than others. In addition, the abundance of the digested proteins plays a role. If a low copy protein shares a spot with a high copy readily ionizing protein, the low copy protein will most probably remain undiscovered. Besides that, we examined the NE proteome of only one cell type – the N2a cells. It is possible that the composition of the NE could be to some extent cell type specific. Therefore, there are certainly more unknown proteins at the nuclear envelope and particularly at the inner nuclear membrane than those seen in our study. Other methods will be required to discover these proteins. An example for that is the KIAA0668, which was found through its similarity to KIAA0810 (see below).

2.1.4 Bioinformatic characterization of LUMA and KIAA0810; KIAA0668 – a third novel protein of the inner nuclear membrane?

After identification of the novel proteins, a more careful data base search was performed. The publicly available data bases were searched for the following information about the new proteins:

- homologues with known function (programs used: BLASTP at http://www.ncbi.nlm.nih.gov/blast/; ClustalW at http://www2.ebi.ac.uk/clustalw; and ESPript2.0 at http://prodes.toulouse.inra.fr/ESPript/)
- phenotype associated with the mutation in the human gene (program used: UniGene at http://www.ncbi.nlm.nih.gov/cgi-bin/UniGene/)
- abundance of the proteins in different tissues (program used: UniGene at http://www.ncbi.nlm.nih.gov/cgi-bin/UniGene/ for LUMA; Kazusa Research Institute at http://www.kazusa.or.jp/huge/ for KIAA0810 and KIAA0668)
- predicted domain structure (programs used: SMART at http://smart.embl-heidelberg.de/smart/ for domain prediction, OMIGA (Oxford Molecular) for hydropathy plots)

The retrieved information was used to design further experiments (especially for LUMA) and to speculate on possible functions of these proteins.

2.1.4.1 LUMA

A BLASTP (Altschul et al., 1997) search using the murine LUMA protein sequence as input yielded following results (Tab. 2-1).

IDENTIFIER	NAME	ORGANISM	LENGTH (No of aminoacid residues)	EXPECT VALUE	IDENTITIES (identical residues/total matched residues)	POSITIVES (identical and similar residues/total matched residues)
gi|12836214	LUMA	Mus musculus	400	0.0		
gi|13236587	hypothetical protein MGC3222	Homo sapiens	400	0.0	93 % 372/400	97 % 388/400
gi|7295182	CG8111 gene product	Drosophila melanogaster	376	3e-46	34 % 122/355	52 % 186/355
gi|13472560	hypothetical protein	Mesorhizobium loti	425	1e-45	33 % 121/360	51 % 189/360
gi|6324398	hypothetical ORF; Ynr070wp	Saccharomyces cerevisiae	1333	0.81	21 % 41/191	37 % 73/191
gi|16330634	probable polysialic acid transport protein KpsM	Synechocystis sp	302	2.1	31 % 19/60	54 % 33/60
gi|16272458	DNA-directed RNA polymerase β' chain (transcriptase β' chain) (RNA polymerase β' subunit)	Haemophilus influenzae	1415	3.7	28 % 33/116	41 % 49/116
gi|7480630	probable DNA polymerase III, α chain	Streptomyces coelicolor	1185	8.9	30 % 21/70	45 % 32/70

Tab. 2-1 BLASTP search using the murine LUMA protein sequence as input. Sequences producing a significant similarity score. All LUMA homologues exist only as predicted proteins in different species. Their functional assignment is based on homology to other proteins with a particular function.

No homologues with a defined or characterized function were found. The polymerases from *Haemophilus influenzae* and *Streptomyces coelicolor* can not be considered as true homologues of LUMA, nevertheless there is some significant similarity in their primary structure. Pairwise alignment reveals similar distribution of clusters of amino acids, which could be a hint at the existence of similar structural features.

The human LUMA gene (annotated as the hypothetical protein MGC3222 (LocusLink 79188)) is located on the chromosome 3. No mutations with a phenotype are known to be associated with this region.

According to UniGene, human LUMA could be found in the following cDNA sources: adipose tissue, adrenal gland, aorta, bladder, blood, bone, brain, breast, cervix, colon, ear, foreskin, genitourinary tract, germ cells, heart, kidney, liver, lung, lymph, lymph node, muscle, normal nervous tissue, nervous tissue from tumors, ovary, pancreas, parathyroid, placenta, testis, pooled pancreas and spleen, prostate, skin, small intestine, stomach, thymus, tonsil, uterus, whole embryo. This clearly suggests that LUMA is an ubiquitously expressed protein found in most tissues.

The domain prediction program SMART (Schultz et al., 1998 and Schultz et al., 2000) did not find any defined domains in the murine LUMA, except for four putative transmembrane segments positioned at amino acids 32–51, 309–331, 346–368, 373–390. These are annotated in the hydropathy plot obtained with OMIGA (fig. 2-6).

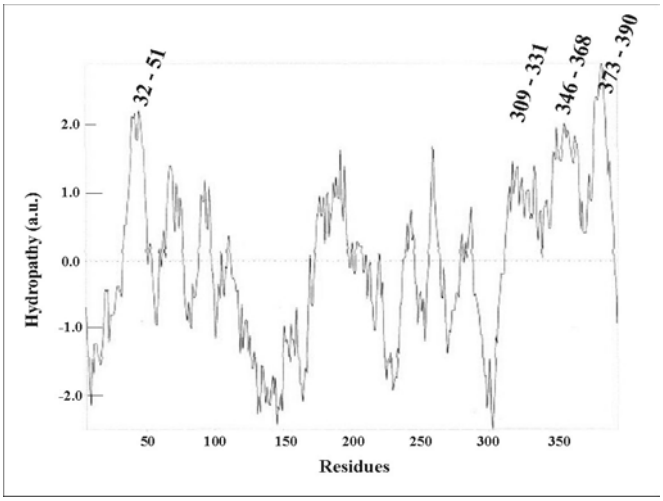

Fig. 2-6 Kyte-Doolittle hydropathy plot for LUMA, window width setting: 11 amino acids. The transmembrane segments predicted by SMART are annotated.

Beside the predicted transmembrane segments, a fifth hydrophobic sequence located between residues 175 and 200 can be seen. The analysis of the nucleic acid sequence of LUMA reveals a remote homology to a PsaJ domain in this region. The PsaJ domain is a protein interaction domain found in the photosystem 1 present in the thylakoid membrane of the chloroplast and cyanobacteria (Fischer et al., 1999). LUMA has most certainly nothing to do with the

photosystem, nevertheless the sequence with the similarity to the PsaJ domain may represent a protein-protein interaction domain.

2.1.4.2 KIAA0810

A BLASTP (Altschul et al., 1997) search using the KIAA0810 protein sequence as input yielded the following results (Tab. 2-2).

IDENTIFIER	NAME	ORGANISM	LENGTH (No of aminoacid residues)	EXPECT VALUE	IDENTITIES (identical residues/total matched residues)	POSITIVES (identical and similar residues/total matched residues)
gi|3882341	KIAA0810	Homo sapiens	824	0.0		
gi|12852531	putative protein	Mus musculus	790	0.0	60 % 499/825	68 % 573/825
gi|6538751	SUN1	Homo sapiens	424	0.0	96 % 409/424	96 % 409/424
gi|14778953	KIAA0668	Homo sapiens	717	1e-79	35 % 207/583	51 % 301/583
gi|6538749	SUN2	Homo sapiens	440	2e-75	43 % 161/371	60 % 225/371
gi|6538738	UNC-84A	C. elegans	1111	1e-42	47 % 91/193	64 % 124/193
gi|13929122	sperm antigen 4	Rattus norvegicus	444	4e-35	37 % 72/192	57 % 111/192
gi|15238380	putative protein	Arabidopsis thaliana	471	2e-20	36 % 71/195	50 % 99/195
gi|1351036	Spindle pole body associated protein Sad1	Schizosaccharomyces pombe	514	1e-17	32 % 62/190	49 % 96/190

Tab. 2-2 BLASTP search using the KIAA0810 protein sequence as input. Selected sequences producing a significant similarity score. KIAA0810 is the SUN1 protein, a human homologue of UNC-84A.

KIAA0810 is the SUN1 protein and a human homologue of UNC-84A. This becomes more clear when looking at the direct alignment (fig. 2-7, two first rows). SUN1 is a putative protein named SUN because of its homology to Sad1 and UNC-84A (Malone et al., 1999). The database entries for SUN1 and SUN2 are not complete. The complete sequences of correct length (as compared to KIAA0810 and KIAA0668) are only mentioned in a publication on UNC-84A (Malone et al., 1999), but were never deposited in the databases.
UNC-84A, in turn, is a characterized *C. elegans* protein with an assigned function. It contains eight putative transmembrane domains (predicted by SMART) and is located at the nuclear

envelope. Mutations in the *unc-84* gene lead to nuclear migration defects and unanchoring of the nuclei. Nuclear migration is essential for the movement of pronuclei during fertilization, for normal mitotic and meiotic cell division and for a variety of interphase functions (Morris et al., 1995). Since nuclear migration is dependent on the presence of intact microtubuli and since the force which produces nuclear movement could act through the centrosome (Raff et al., 1989), Malone et al. propose that UNC-84A is most probably an integral nuclear envelope protein involved in the interaction between the centrosome and the nucleus. It is unclear whether this function is conserved in SUN1. Apart from the proteins listed in table 2-2, a number of structural proteins, like myosin, vimentin or kinesin were found to have some similarity to KIAA0810. This could indicate that KIAA0810/SUN1 is a structural protein and could also have a role in anchoring of the centrosome in humans. Centrosome engulfment in the nuclei was recently described by Salina et al. (2002). According to this article, centrosomes localize to the invaginations of the nuclear envelope in a microtubule–dependent process. The detailed mechanism of recruitment and attachment of microtubuli and of the centrosomes to the NE is still unknown. SUN1 and probably SUN2 as well are good candidates for the anchoring of the centrosome during mitotic nuclear breakdown.
Because of its involvement in the interaction between the centrosome and the nucleus, UNC-84A was suggested to be an outer nuclear membrane protein. In contrast, we propose that KIAA0810 is an inner nuclear membrane protein because of its resistance to extraction with Triton X-100 and the immunofluorescence signal giving rim-like staining around the nucleus (Dreger et al., 2001). Only electron microscopy can bring absolute clarity to this question, but the interaction between the centrosome and the nucleus is not an argument against INM localization of KIAA0810 (see above). Furthermore, KIAA0810 possesses a DNA-binding domain (see below) which is another argument for an inner nuclear membrane localization of this protein.

Apart from UNC-84A, another KIAA clone was found to have a great similarity to KIAA0810, namely the KIAA0668. KIAA0668 is the human protein SUN2 (alignment fig. 2-7, compare 3rd and 4th row) and another novel integral membrane protein of the inner nuclear membrane (see 2.1.4.3 and 2.1.5).

According to the UniGene program, the KIAA0810 gene (LocusLink 23353) is located on the human chromosome 7.

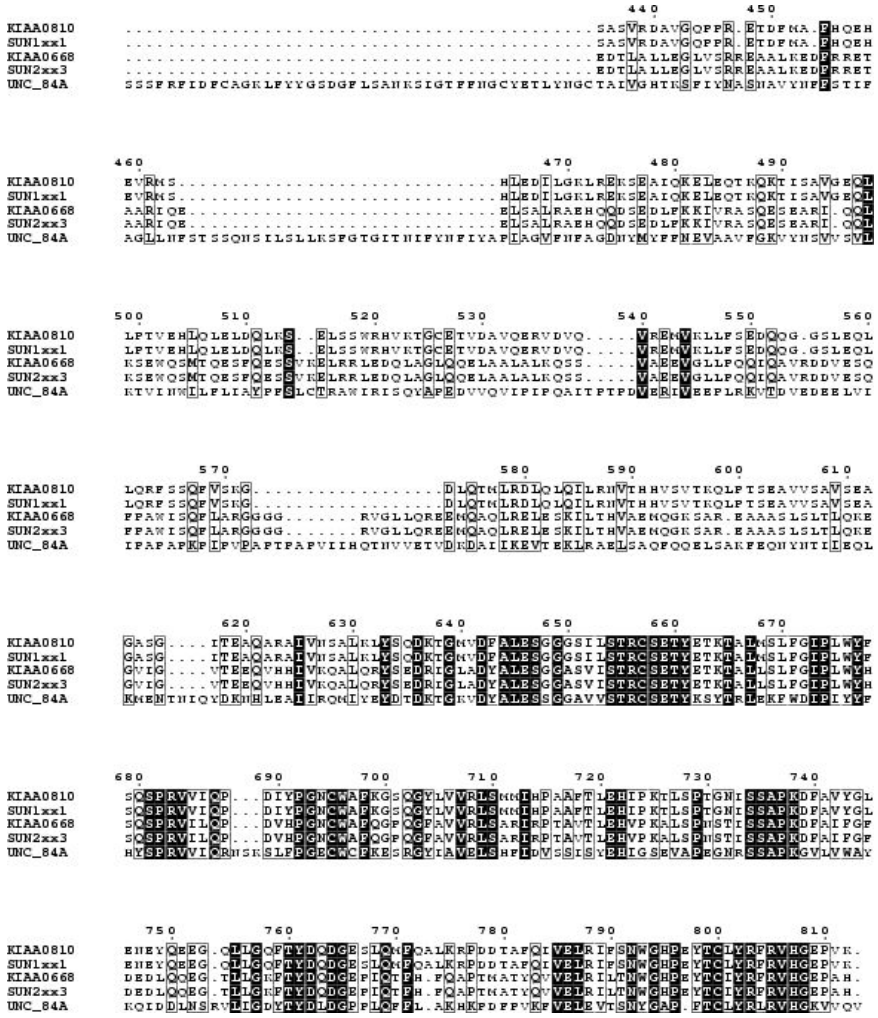

Fig. 2-7 Alignment of the C-termini of KIAA0810, KIAA0668, SUN1, SUN2 and UNC-84A. The alignment was made using ClustalW and was edited with ESPript. Marked in black are the identical amino acids, conserved amino acid exchanges are in the boxes. Note the pairwise identity between KIAA0810 and SUN1 and KIAA0668 and SUN2.

KIAA0810 cDNA could be found in following cDNA sources (according to UniGene): adipose tissue, adrenal gland, amnion normal, aorta, blood, bone, bone marrow, brain, breast, colon, ear, esophagus, eye, foreskin, germ cell, head and neck, heart, kidney, kidney tumor, lung, lymph, muscle, normal nervous tissue, nervous tissue from tumors, ovary, pancreas, parathyroid, placenta, pooled lung and spleen, prostate, skin, smooth muscle, stomach, testis, thyroid, tonsil, uterus, whole embryo.

Additionally, the expression information obtained from Kazusa revealed that KIAA0810 is expressed at a low level in all tissues and at a very low level in spleen.

According to SMART, human KIAA0810 contains two putative transmembrane segments positioned at amino acids 287–309 and 316–335. These are annotated in the hydropathy plot (fig. 2-8). Additionally, SMART predicts two protein – protein interaction domains (coiled coil structures) positioned at amino acids 404–429 and 455–493 and a BRLZ domain (amino acids 466–528). The BRLZ domain was found just above the significance threshold, but was judged as relevant, because of its function. BRLZ stands for 'basic region leucine zipper' and is found in DNA binding proteins. In these proteins, a basic region mediates the sequence specific DNA binding, followed by a leucine zipper structure required for dimerization. Whether this BRLZ domain is functional has to be experimentally confirmed.

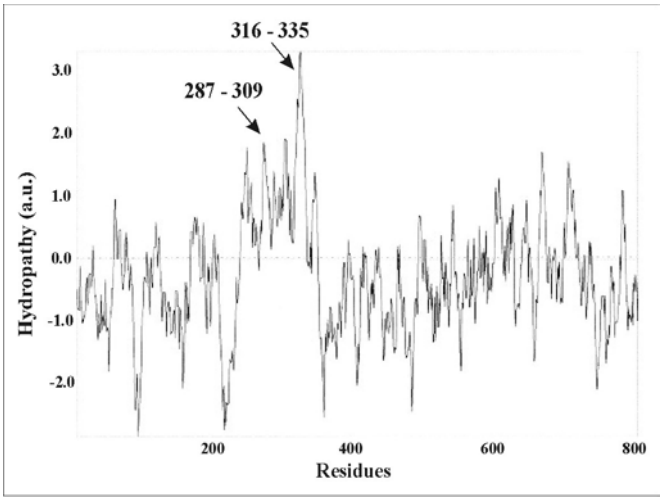

Fig. 2-8 Kyte-Doolittle hydropathy plot for KIAA0810, window width setting: 11 amino acids. The transmembrane segments predicted by SMART are annotated.

Interestingly, according to SMART, the murine KIAA0810 contains a C2H2 zinc finger domain and three putative transmembrane segments. The zinc finger domain resembles that of nucleic-acid binding proteins and is located at the amino acid residues 183–205.
This could mean that the murine KIAA0810 contains two DNA binding domains. It would be interesting to compare the expression patterns of the murine KIAA0810 and the human protein. The additional zinc finger may alter the function of the murine protein as compared with the human protein, which may result in increased level of its expression.

2.1.4.3 KIAA0668

KIAA0668 was found by a BLASTP search as a homologue of KIAA0810. The C-terminal part of its sequence has been annotated in public databases as SUN2. No other homologues or predicted functions are known.

According to the UniGene program, the KIAA0668 gene (LocusLink 25777) is located on the human chromosome 22 (cytogenetic: 22q13.1) and could be found in the following cDNA sources (according to UniGene): B-cells, eye, pancreas, adrenal gland, amnion normal, bladder, blood, bone, brain, breast, colon, esophagus, foreskin, genitourinary tract, germ cell, head and neck, heart, kidney, kidney tumor, lung, marrow, muscle, normal nervous tissue, nose, ovary, parathyroid, placenta, pooled brain, lung, testis, pooled lung and spleen, pooled pancreas and spleen, prostate, skin, small intestine, stomach, testis, thymus, thyroid, tonsil, uterus, uterus tumor, whole embryo.
Additionally, the expression information obtained from Kazusa revealed that KIAA0668 is expressed in all tissues at a moderately high level, and at a particularly high level in heart, brain, testis and ovary.

According to SMART, human KIAA0668 contains two putative transmembrane segments positioned at amino acids 205–227 and 239–261. These are annotated in the hydropathy plot (fig. 2-9). Additionally, SMART found two protein – protein interaction domains (coiled coil structures) positioned at amino acids 430–461 and 501–528 and a BRLZ domain (amino acids 431–481).

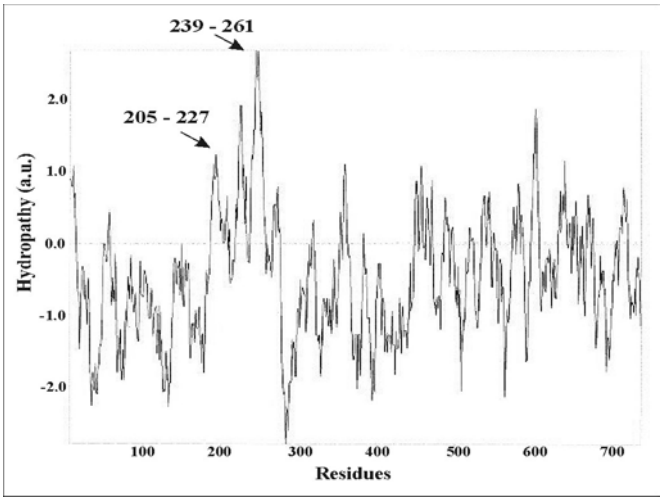

Fig. 2-9 Kyte-Doolittle hydropathy plot for KIAA0668, window width setting: 11 amino acids. The transmembrane segments predicted by SMART are annotated.

KIAA0668 is structurally very similar to the KIAA0810. Both proteins contain two putative transmembrane segments and the same protein/DNA interaction domains located in the C-terminal part of the protein. A comparison of the domain structures in UNC-84A, KIAA0810 and KIAA0668 is found as a schematic presentation in the fig. 2-10.

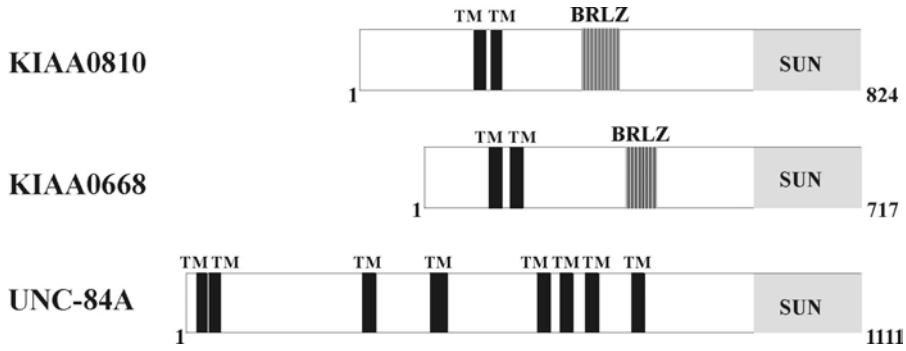

Fig. 2-10 Domain structure of KIAA0810, KIAA0668 and UNC-84A. Each protein contains predicted transmembrane sequences (TM). KIAA0810 and KIAA0668 contain a DNA-binding BRLZ domain which is absent in UNC-84A. The region of identity shared by all three proteins is the SUN domain (marked in grey). Note the similarity in the domain arrangement between KIAA0810 and KIAA0668.

2.1.5 Localization of KIAA0668 in COS-7 cells and its biochemical characterization

In analogy to KIAA0810, the DNA coding for the KIAA0668 was amplified by PCR from its cDNA clone yielding a 2200 bp fragment. This fragment was also cloned into the pcDNA3.1/V5-His vector. The plasmid was transfected into COS-7 cells and the distribution of the expressed protein was examined by immunofluorescence microscopy using the anti-V5 antibody.

Just as for KIAA0810 and LUMA, the indirect immunofluorescence detected by confocal laser scanning microscopy (fig. 2-11) revealed a rim-like fluorescence pattern around the nucleus typical for integral membrane proteins of the INM. Thus, KIAA0668 is another novel integral membrane protein of the INM.

Fig. 2-11 Overexpression of KIAA0668 in COS-7 cells. Overexpressed KIAA0668 gives rise to a rim-like staining around the nucleus as visualized by indirect immunofluorescence: COS-7 cells were transfected with a V5-tagged KIAA0668 cDNA plasmids. Immunofluorescence studies were carried out with permeabilized cells grown on glass cover slips, as described in Methods.

Since KIAA0668 was not detected by the proteomic approach, nothing was known about its interaction with the lamina. Fortunately, an antibody against SUN2 already existed (kindly provided by Didier Hodzic, University of Washington, St.Louis, USA) and could be used for the biochemical characterization. NE were prepared and extracted with TX-100, the pellet, supernatant and the total NE were separated on SDS-PAGE and immunoblotted (fig. 2-12). The INM marker LAP 2β was found in the original NE preparation and in the TX-100 resistant fraction. In contrast, most of the ONM/ER marker calnexin could be extracted with TX-100 and was thus found in the supernatant. As expected, the antibody against SUN2 recognized a protein with an apparent molecular mass of ~80 kDa. Similar to LAP 2β, this band was present in the original NE preparation and in the TX-100 resistant fraction. This indicates that SUN2 probably interacts with the lamina and, since it is a putative transmembrane protein, it should be an integral membrane protein of the INM.

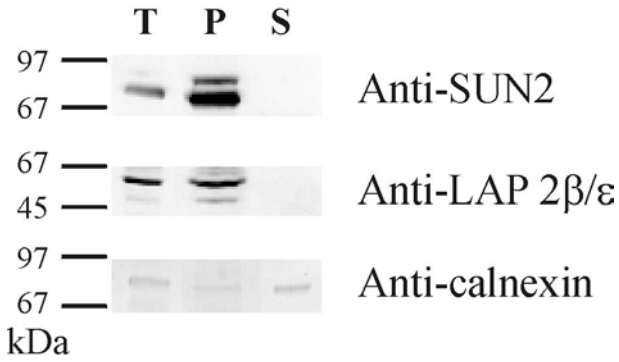

Fig. 2-12 Biochemical characterization of KIAA0668, Western blot. Nuclear envelopes from N2a cells were extracted with TX-100 and the fractions were analyzed for the presence of SUN2 and marker proteins LAP 2β/ε for INM and calnexin for ER. T: total NE; P: pellet after TX-100 extraction; S: supernatant after TX-100 extraction.

In a coimmunoprecipitation experiment peformed by D. Hodzic, KIAA0668 coprecipitated with lamin B1, thus confirming the postulated lamina interaction and the validity of the TX-100 extraction approach. The INM localization of KIAA0668 was verified beyond any doubt by electron microscopy (D. Hodzic, personal communication).

2.2 FUNCTIONAL CHARACTERIZATION OF LUMA

Data base searches showed that LUMA is a protein, that is completely different from any INM protein characterized so far. We therefore decided to concentrate our efforts on the functional characterization of LUMA. We assumed that studying LUMA might reveal new aspects of nuclear envelope functions.

We performed an overexpression experiment and took a closer look at LUMA`s immunofluorescence. As it turned out, overexpression of LUMA had unusual effects on the cells. The NE appeared 'swollen' in transfected cells and had vesicle–like structures attached (fig. 2-13). Also the chromatin seemed 'less dense' in transfected cells as compared to the control cells.

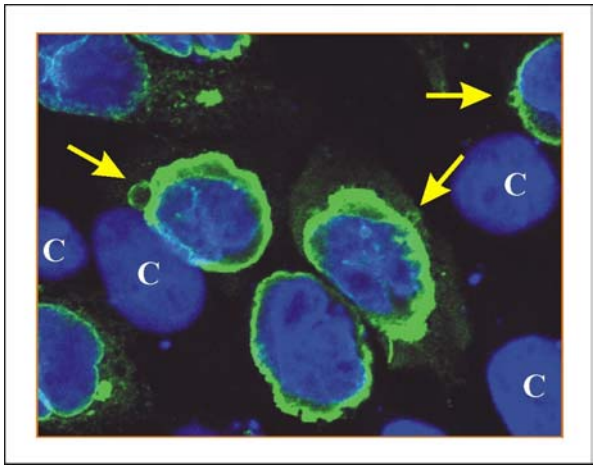

Fig. 2-13 Overexpression of LUMA in COS-7 cells. The V5-tagged LUMA is visualized by the immunofluorescence using the anti-V5 antibody (green stain), chromatin is stained by DAPI (blue). Note the 'swollen' appearance of the NE, the vesicle-like structures at the NE (marked with arrows) and the 'less dense' appearance of the chromatin as compared to the untransfected control cells in the same displayed area (marked with C).

2.2.1 Overexpression of LUMA in COS-7 cells – comparison with other INM proteins

The morphology of the cells overexpressing LUMA is different from the morphology observed when other INM proteins are overexpressed. To have a direct comparison, lamin B receptor (amplified from its cDNA) and lamin B2 (amplified from N2a cell cDNA) were cloned into appropriate vectors and overexpressed by transient transfection of COS-7 cells.

The localization of the proteins was visualised by immunofluorescence and checked for colocalization with the endogenous LAP 2β/ε immunofluorescence. The results are summarized in fig. 2-14. Overexpression of lamin B receptor leads to the formation of invaginations into the nucleus (fig. 2-14 A), and overexpression of lamin B2 caused vesicle formation at the NE towards the inside of the nucleus (fig. 2-14 E). Overexpression of LUMA on the other hand, caused swelling of the NE and vesicle or aggregate formation outside the nucleus (fig. 2-14 C). While the lamin B2 colocalizes with the LAP 2β/ε signal only to a minor extent at the interphase between INM and lamina (fig. 2-14 F), the immunofluorescence signal of the integral INM protein lamin B receptor shows the expected colocalization. Similarly, LUMA colocalizes with LAP 2β/ε (fig. 2-14 D), which can be seen as another evidence for its INM localization. In contrast, the deformation of the nuclear membrane caused by LUMA is different from the one caused by the lamin B receptor (no invaginations). The invaginations are long deep membrane channels reaching into the inside of the nucleus with cytoplasm extending into them (Fricker et al., 1997). Lamin B receptor interacts with nucleosomal linker DNA and the chromodomain protein HP1 (Ye Q, et al., 1997). These interactions are probably responsible for the recruitment of chromatin to the INM and the formation of invaginations. Since such invaginations are absent when LUMA is overexpressed (fig. 2-14 A), a potential interaction of LUMA with the chromatin must be of different nature from that of the lamin B receptor.

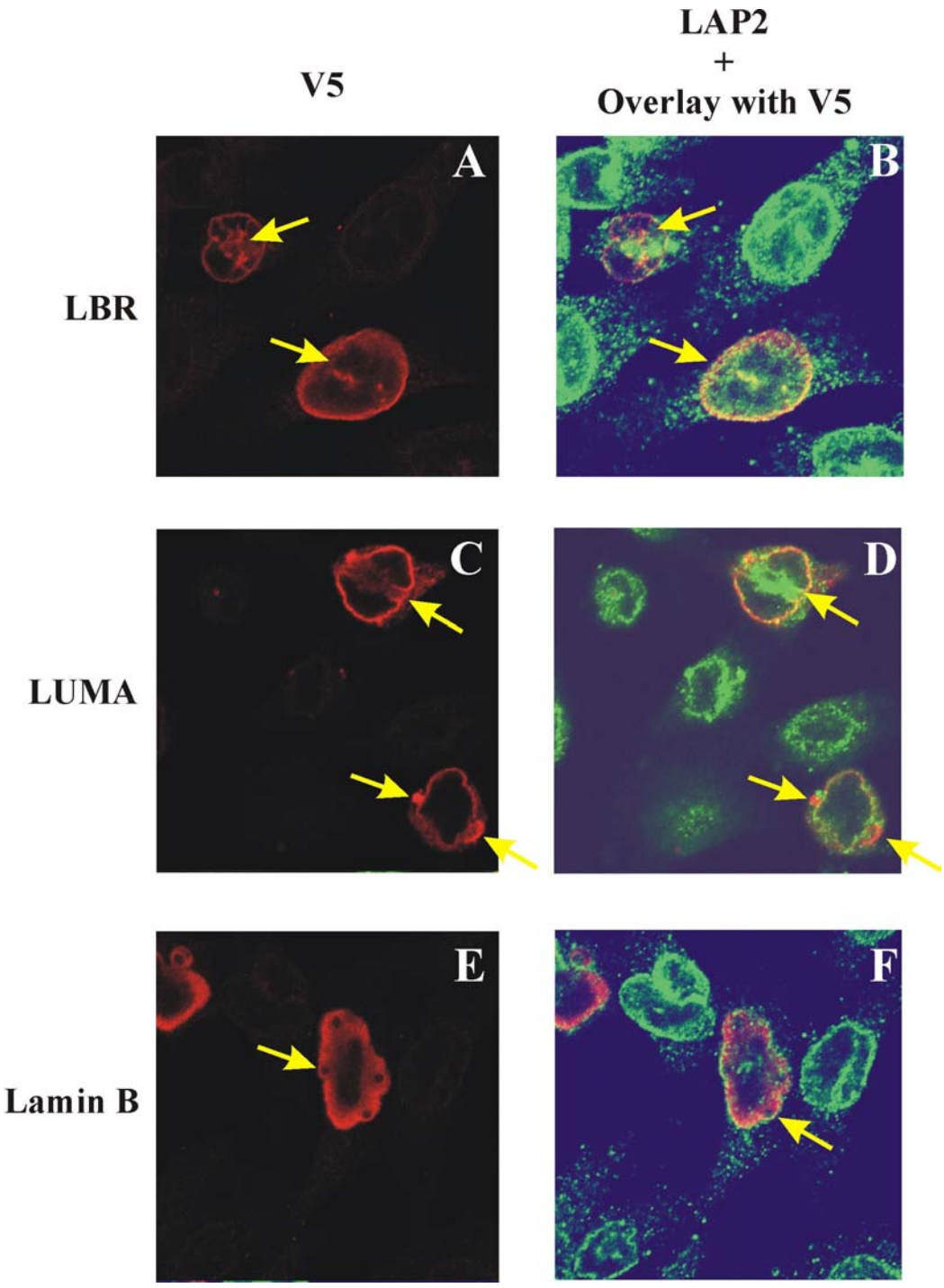

Fig. 2-14 Comparison of the effect of overexpression of lamin B receptor, LUMA and lamin B2 in COS-7 cells and of their colocalization with endogenous LAP 2β/ε. The overexpressed proteins are presented in red using the anti-V5 antibody immunofluorescence, endogenous LAP 2β/ε is presented in green and colocalization in yellow. The characteristic features discussed in the text are marked with arrows. The dotted appearance of the LAP 2β/ε immunofluorescence is caused by the Cy2-conjugated anti-rabbit-IgG secondary antibody.

2.2.2 Localization of LUMA deletion mutants – inner nuclear membrane targeting domain and topology of LUMA

After demonstrating that LUMA is a protein of the INM, two further questions were addressed: first, what is the topology of LUMA and second, is there a defined part of the protein which is responsible for its INM localization (an 'inner nuclear membrane targeting sequence')? We were most interested in knowing which part of the protein is oriented towards the nucleoplasma and whether the predicted transmembrane segments are real. Knowing the position of an inner nuclear membrane targeting sequence would give a hint to the position of potential protein- or DNA-interaction domains within the sequence of LUMA. Both questions could be answered, at least partially, by expressing LUMA deletion mutants in COS-7 cells. Since nothing was known about the domain structure of LUMA, the deletion mutants were constructed simply by dividing the protein into equal halfs or at boundaries of the putative transmembrane segments (fig. 2-15).

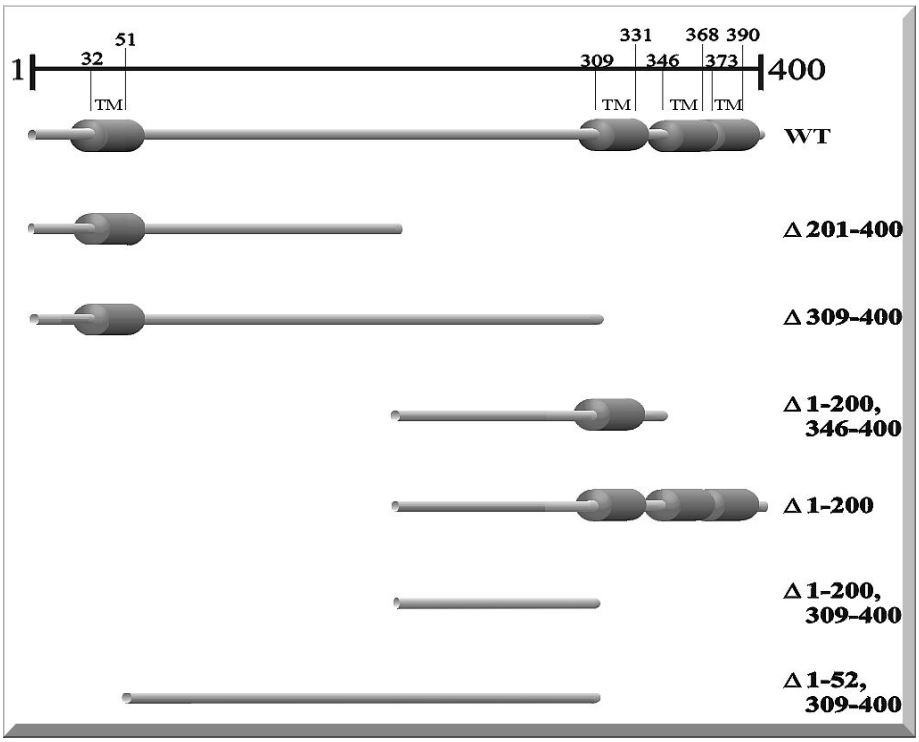

Fig. 2-15 Constructed LUMA deletion mutants. The scale above refers to the length of the protein in amino acids, TM transmembrane region, WT wild type.

The fragments were cloned into pcDNA3.1(-)myc/His vector which supplied the mutant protein with a C-terminal myc and His_6 tag. The proteins were expressed in COS-7 cells and

their distribution was examined by immunofluorescence microscopy using the anti-myc antibody (fig. 2-16). The localization of the proteins was judged relative to the localization of the endogenous LAP 2β/ε.
Generally, it was observed that the less of LUMA was deleted, the better it colocalized with LAP 2β/ε. Also, the greater the part of LUMA that was expressed, the more cells seemed to survive the overexpression. This can be clearly seen in fig. 2-16 C, which shows the subcellular distribution of the deletion mutant missing only the last three predicted transmembrane segments.

Overexpression of the N-terminal half of protein (fig. 2-16 A) led to the formation of invaginations, which are similar to invaginations formed when fragments of lamin B receptor are overexpressed (Ellenberg et al., 1997). Also, the ER was overloaded with the protein which is again similar to what one observes when overexpressing the lamin B receptor. This could indicate, that N-terminal parts of LUMA and the lamin B receptor could be involved in maintaining the structural integrity of the NE in a similar way.

Overexpression of the C-terminal part of LUMA had a dramatic effect on the morphology of the transfected cells. Aggregates were formed and very few cells survived (fig. 2-16 D). Interestingly, the aggregates also contain LAP 2β/ε, since a clear colocalization could be observed. Native LUMA contains four putative TM sequences, which are probably clustered in the membrane. Taking away one segment and increasing the concentration of the remaining three may lower the threshold for aggregation. The formed aggregates distort the whole NE structure, maybe simply by physical stretching and pulling of the membrane, similar to the events during the mitotic prophase (Beaudouin et al., 2002). Other INM proteins like LAP 2β/ε also get concentrated at the LUMA aggregates that way, an effect which can be seen in fig. 2-16 D.

The deletion mutant LUMA Δ1-200,346-400 was the smallest part of LUMA still localizing to the INM (fig. 2-16 B). Thus, amino acids 201-345 of LUMA are sufficient for its INM localization.

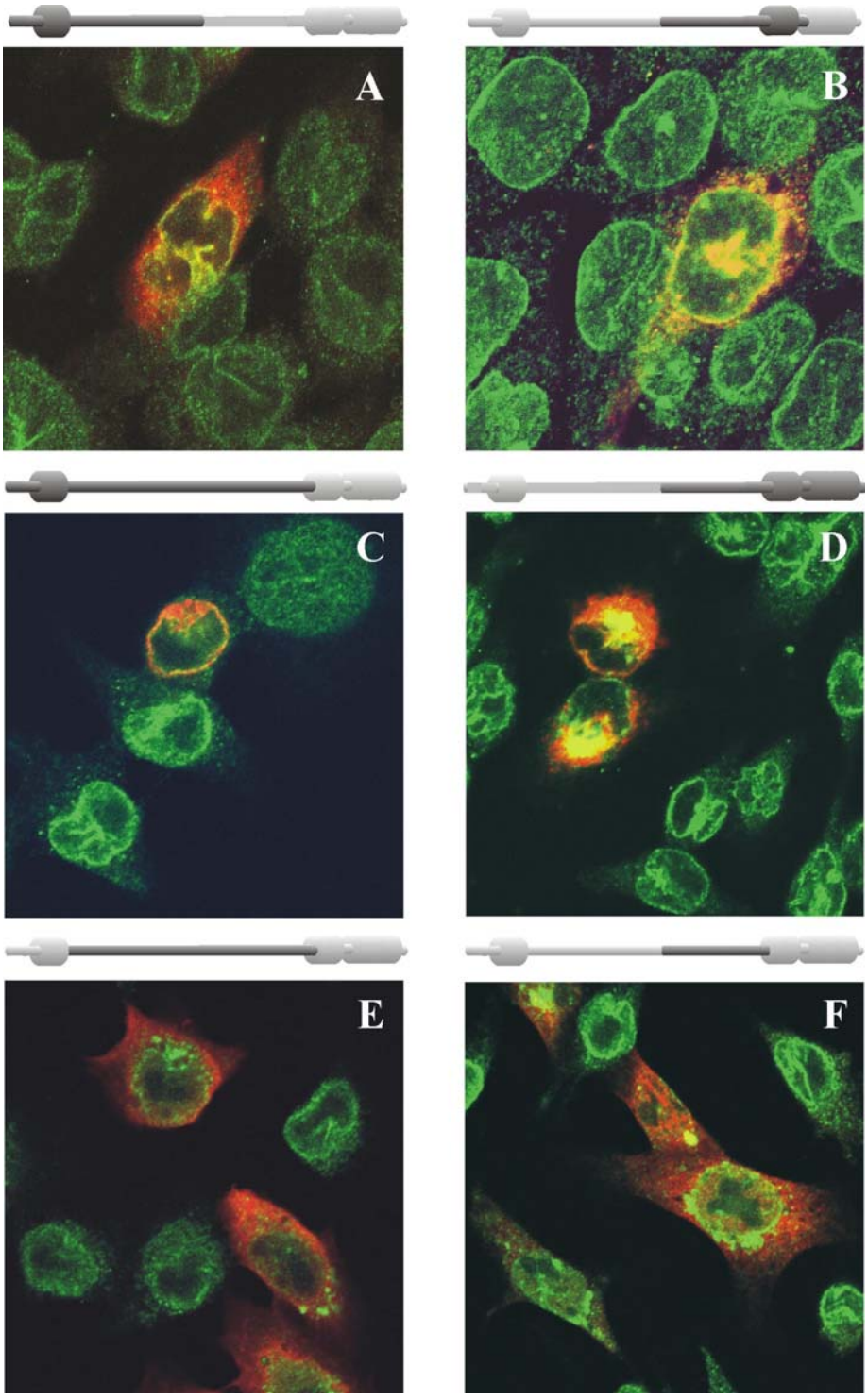

Fig. 2-16 Overexpression of LUMA deletion mutants and their colocalization with endogenous LAP 2β/ε in COS-7 cells. The overexpressed proteins are presented in red, endogenous LAP 2β/ε in green and colocalization in yellow. The bars above the micrographs marked in dark indicate the parts of protein which are expressed. The dotted appearance of the LAP 2β/ε immunofluorescence is caused by the Cy2-conjugated anti-rabbit-IgG secondary antibody.

The presence of at least one transmembrane segment is essential for nuclear membrane localization, as could be seen when overexpressing the soluble fragments. The amino acid sequence of LUMA located between the first and second putative transmembrane sequence appeared to be actively exported from the nucleus (fig. 2-16 E). Since the fragment has a molecular weight of 33kDa, it should be able to passively diffuse into the nucleus and become equally distributed between cytoplasm and nucleus. This is not the case. Judged from the immunostaining, the putative nucleoplasmic loop can be only found in the cytoplasm. Since the structure of the NE is distorted, the expressed fragment must have entered the nucleus, but since it is not detectable there, it must have been actively exported back to the cytoplasm. The most probable explanation for this observation is a tight regulation of the amount and the localization of LUMA in the nucleus. The putative nucleoplasmic loop has probably an important function (see also 2.2.4) and the cell cannot afford to its free diffusion within the cell and the accumulation in excess amounts.

A similar, but less dramatic effect could be observed when the LUMA Δ1-200,309-400 was overexpressed (fig. 2-16 F). This fragment was apparently able to diffuse into the nucleus, but was still excluded from some structures. Inside the nucleus, it seems to concentrate at the NE. The majority of the protein can be found in the cytoplasm, probably due to the same reasons as discussed above for the whole nucleoplasmic loop. It might be too short to be fully functional, which could be the reason why it is tolerated to some extent in the nucleus, although the whole NE becomes heavily distorted in cells overexpressing this mutant (as judged from the distribution of LAP 2β/ε). This is also the part of LUMA which is minimally required for the nuclear interactions needed for the INM localization of the whole protein.

The main conclusion from these experiments, is that maintaining a normal expression level of the full length LUMA protein is crucial for the structure and integrity of the NE.

As to the topology of LUMA, the deletion mutant experiments indicate, that both N- and C-terminus are located in the ER lumen. The existence of first and second transmembrane sequence at the predicted positions could be shown (fig. 2-16 A, B), also the solubility of the loop separating these membrane-spanning sequences could be demonstrated (fig. 2-16 E, F). The strongest support for the orientation of the soluble loop between first and second transmembrane region towards the nucleus comes from the localization experiment with the deletion mutant LUMA Δ1-200,346-400 (fig. 2-16 B). This fragment clearly localizes to the INM. According to the current theory about how the proteins of the INM find the way to their

final destination, such proteins diffuse around in the ER, ONM and INM until they find interaction partners in the nucleus and are anchored there (Ellenberg et al., 1997). The only piece of protein available for interaction in LUMA Δ1-200, 346-400, is its N-terminal part (before the TM segment), therefore it has to point towards the nucleus.
The proposed topology of LUMA is summarized in fig. 2-17.

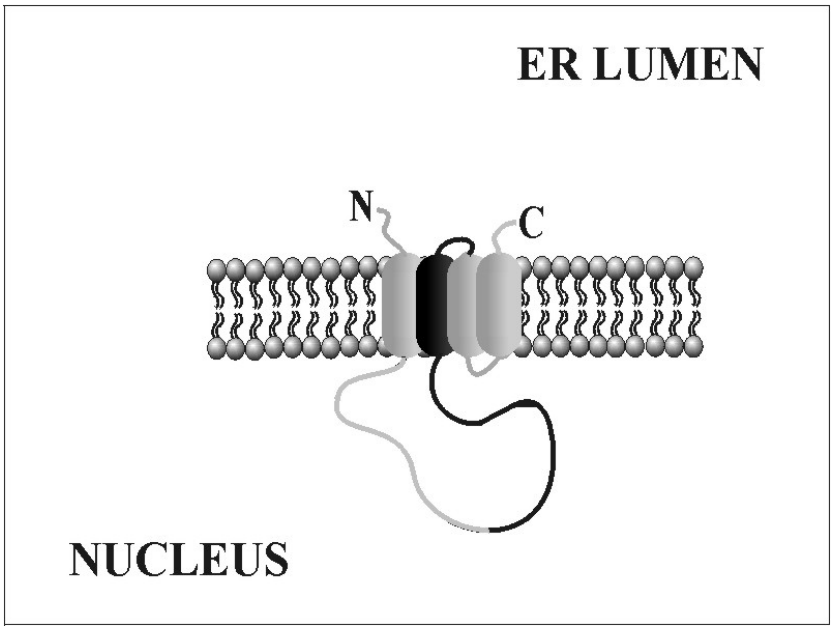

Fig. 2-17 The suggested transmembrane topology of LUMA. The loop between the first and second transmembrane segment is pointing towards the nucleus. The minimal sequence sufficient for the inner nuclear membrane localization is highlighted in black.

2.2.3 Downregulation of LUMA in 3T3 cells

Having too much of LUMA is obviously problematic for the cells, but what happens if the expression of LUMA is downregulated? To answer this question, an anti-sense approach was used. The purpose of the first part of the experiment, the 'messenger primer walking', was to determine which part of the LUMA mRNA is suited best for the hybridization with an anti-sense oligonucleotide. The next step was to bring the chosen oligonucleotide into the cells and examine its effect on the nuclear morphology. The morphology of the NE was observed by staining for endogenous LAP 2β/ε and by DAPI staining of DNA. Unfortunately, the downregulation of expression of LUMA could not be quantified, since there is no antibody against this protein available yet. Therefore, the results have to be considered as preliminary.

2.2.3.1 Messenger primer walking

The *in vitro*-translated cDNA of LUMA (1200 bp) was incubated with diverse anti-sense oligonucleotides and digested with RNase H. RNase H cleaves only the mRNA structures which have effectively hybridized with the oligonucleotide DNA. The most effective digestion could be observed for the anti-sense oligonucleotides made against the bases 245–263 and bases 802-820 of the cDNA sequence of LUMA (fig. 2-18).

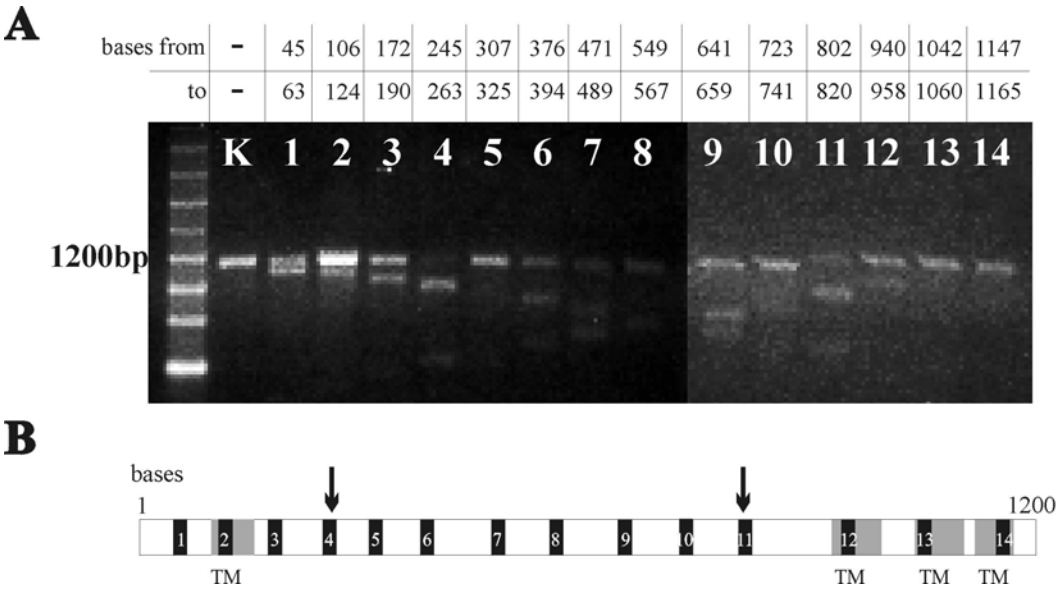

Fig. 2-18 Messenger primer walking. LUMA mRNA was incubated with oligonucleotides designed to hybridize with the mRNA about every 100 bases. The oligonucleotides hybridizing best are those, which resulted in the best removal of mRNA by digestion with RNaseH. **A:** The mRNA fragments resulting from digestion were separated on a denaturing agarose gel. The numbers above correspond to the positions of anti-sense oligonucleotides. K: full length LUMA mRNA; best hybridizing oligonucleotides were: oligonucleotide number 4 hybridizing with bases 245-263 and oligonucleotide number 11 hybridizing with bases 802-820. **B:** Position of anti-sense oligonucleotides relative to the putative transmembrane segments of LUMA. The best hybridizing oligonucleotides are both located on the putative nucleoplasmic loop. Numbers correspond to the oligonucleotide numbers in A. TM: transmembrane regions, marked in grey. The best hybridizing oligonucleotides are marked with arrows.

2.2.3.2 Transfection of anti-sense oligonucleotides into 3T3 cells

Both oligonucleotides were transfected into mouse 3T3 cells, which were then immunostained with anti-LAP 2β/ε antibody 12 hours past transfection. The control cells were treated exactly the same, except that they did not receive any DNA. The oligonucleotide hybridizing with the bases 802-820 of LUMA mRNA produced a phenotype markedly different from the control cells. The oligonucleotide hybridizing with the bases 245-263 of LUMA mRNA induced a similar phenotype, but here it was not as clear as in case of the other oligonucleotide, and could only be observed in very few cells.

The results are shown in fig. 2-19. Just like overexpression, downregulation of LUMA caused the cells to form vesicle–like structures outside the NE. These structures are apparently surrounded by a membrane containing LAP 2β/ε and enclose chromatin, as deduced from the DAPI stain. Additionally, the chromatin structure inside the nucleus is altered as compared to the control cells. The affected nucleus seems to have areas almost void of DNA or alternatively contains overall less DNA. Additionally, a strongly reduced staining intensity indicates that the level of expression of LAP 2β/ε is reduced.

The anti-sense experiment was repeated by Henning Otto by microinjecting the oligonucleotides directly into the cells instead of transfecting them with activated dendrimer/DNA complexes. The results were similar to those described above. Additionally, the microinjected cells sometimes formed thin DNA bridges with the nuclear DNA and LAP 2β - containing vesicles outside the nucleus.

It is difficult to interpret the obtained results. Somehow, LUMA has something to do with the regulation of the chromatin structure, and perhaps with its regulation throughout the cell cycle. Also, loss of LUMA seems to influence the level of expression of other INM proteins indicating a rather fundamental role for LUMA in the functional organization of the NE.

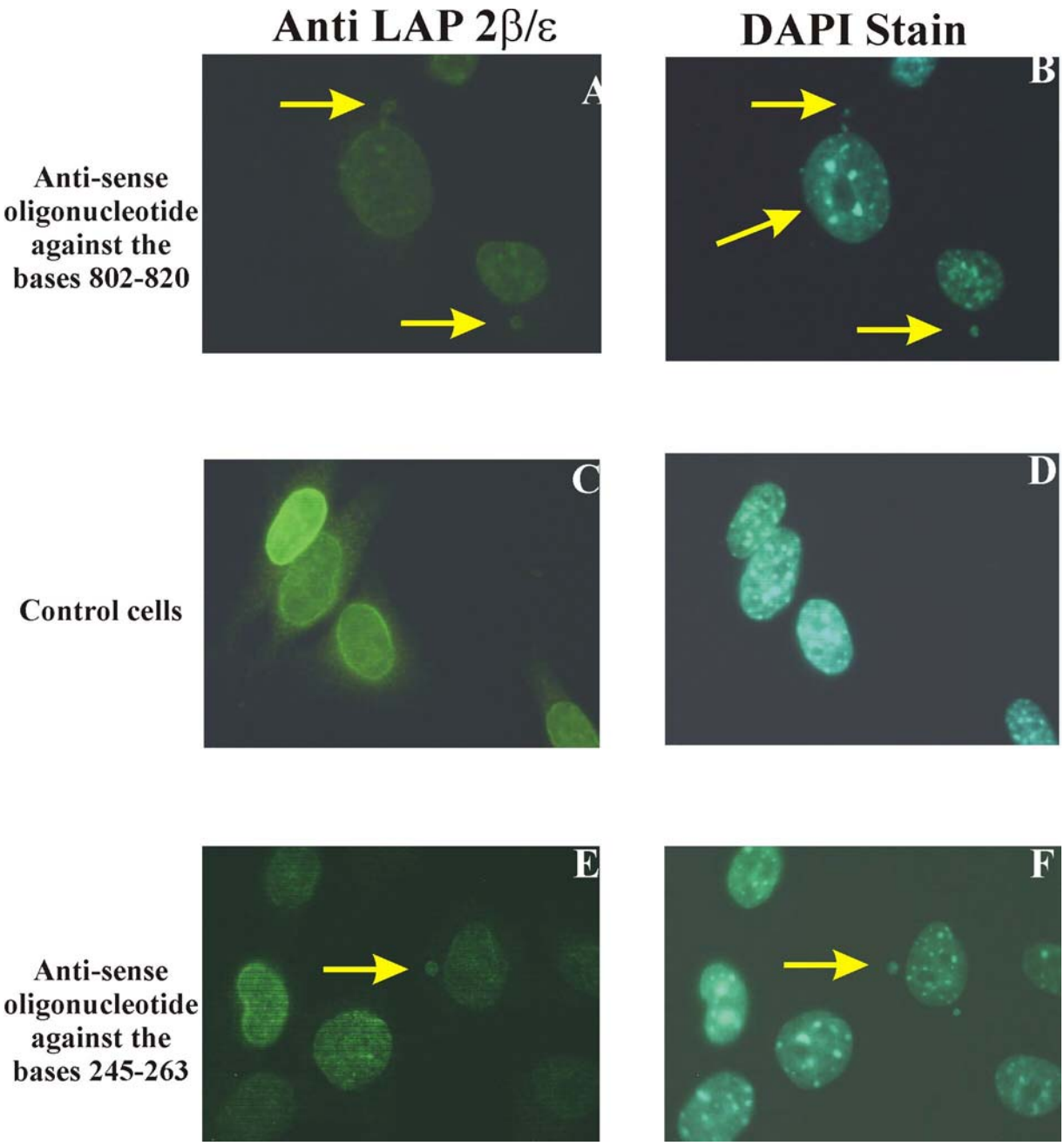

Fig. 2-19 Downregulation of LUMA in 3T3 cells with the anti-sense oligonucleotides against bases 802-820 (A, B), bases 245-263 (E, F) and control cells (C, D). Downregulation of LUMA causes the formation of vesicle–like structures. These structures contain chromatin and are enclosed by a membrane containing LAP 2β/ε. The features discussed above are marked with arrows. Each picture is representative.

2.2.4 Chromatin binding assay

The downregulation experiments suggested that LUMA is somehow involved in the regulation of the chromatin structure. To elucidate LUMA`s role in this process, we wanted to know if LUMA is able to bind to chromatin. For that purpose, a centrifugation assay was performed (see fig. 2-20).

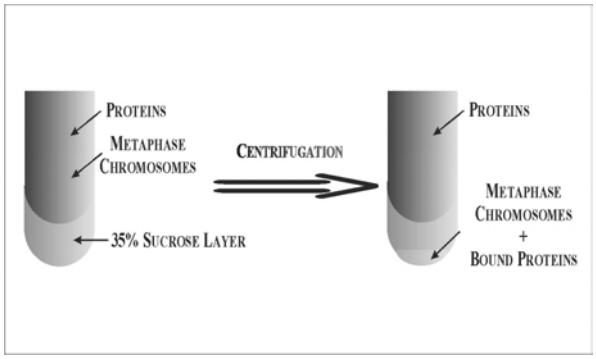

Fig. 2-20 Chromosome binding assay - schematic representation. Recombinantly produced protein was incubated with metaphase chromosomes and centrifuged through a dense sucrose layer. Protein bound to the chromosomes is then found in the pellet fraction.

Metaphase chromosomes were prepared from CHO cells, incubated with LUMA recombinantly produced in *E.coli.* The mixture was then centrifuged through a 35% dense sucrose layer. As a control, a recombinantly produced LAP 2β deletion mutant lacking the transmembrane domain (LAP 2β 1-410) was used. The results are shown in fig. 2-21.

LAP 2β (1-410) clearly binds chromosomes as expected. It was only found in the pellet fraction when the chromosomes were added. In contrast, LUMA could not be detected in any pellet fraction. Normally, this would mean that the examined protein does not bind chromosomes. In the case of LUMA however, no chromosomal pellet was found. Incubation with LUMA apparently caused decondensation of the chromosomes, so that they were not dense enough to sediment through the 35% sucrose layer. This finding indicates that LUMA interacts with chromosomes and that this interaction causes their decondensation or digestion.

It is not clear whether LUMA causes the decondensation directly or indirectly via an associated protein which causes the decondensation. It is conceivable that an interacting protein originates from either the chromosomal preparation or the bacteria used for the purification of the recombinant protein. The observed decondensation must be in any case

LUMA specific, since both LUMA and LAP 2β were purified by the same method from the same bacterial strain, both LUMA and LAP 2β were incubated with the same chromosome preparation and LAP 2β does not cause chromosome decondensation.

The chromosome decondensing property of LUMA explains the lower density of chromatin in cells overexpressing LUMA, as judged from DAPI staining. Also the dilated ER/NE lumen in such cells can be explained by such an effect. The decondensation of chromatin probably leads to a massive upregulation of protein expression and somehow to defects in the secretory pathway. The synthesized protein accumulates in the ER and the ER/NE lumen becomes dilated (a process described for yeast by Matynia et al., 2002). This hypothesis could be tested by following the rate of protein synthesis in cells overexpressing LUMA and looking for the fate of the newly synthesized proteins. Also, the effect of LUMA on gene replication and transcription is relatively easy to test by tracking the incorporation of bromodeoxyuridine (BrdU) in newly synthesized DNA or of bromouridine (BrU) into RNA, respectively.

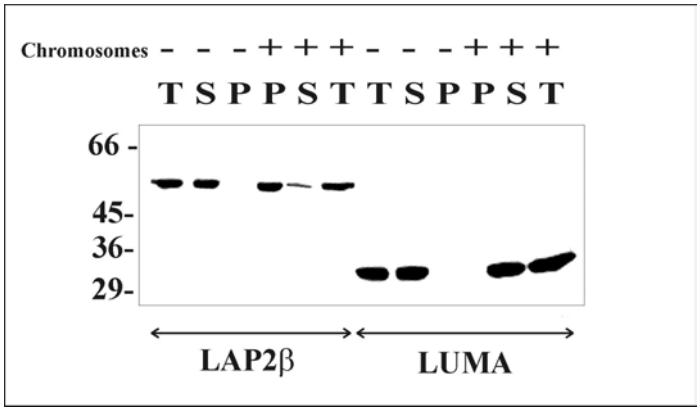

Fig. 2-21 Chromosome binding assay – results. According to the Western blot shown above (myc-tagged LUMA and LAP 2β were stained with anti-myc antibody and horseradish peroxidase conjugated anti-mouse-IgG secondary antibody) LAP 2β binds chromosomes, LUMA does not (compare pellet fraction P plus chromosomes for LUMA and LAP 2β). However, there was no pellet in the sample containing LUMA and chromosomes, so clearly the chromosomes were decondensed and this decondensation was caused by LUMA. P: pellet, S: supernatant, T: total.

2.2.5 Concluding remarks on LUMA

Combining the results from anti-sense and chromatin binding experiments, an attractive speculation on the function of LUMA can be made: cells lacking LUMA may be unable to decondense specific parts of their chromatin and may thus be incapable of replicating those parts during the S phase of the cell cycle. The cells still could pass the G2 phase and complete an impaired mitosis. The parts of chromatin which became replicated would somehow be capable of recruiting INM proteins and with them the nuclear membranes (Buendia et al., 2001). In addition to the main nucleus, a mini nuclear envelope enclosing mininuclei may form and would appear in the cell as a vesicle-like structure containing chromatin. Apparently, no cytokinesis should take place, so that the affected cells end up having two 'nuclei': one normal sized with altered chromatin structure and one or more mini nuclei - the vesicle-like structures.

This hypothesis predicts an exciting role for LUMA in the regulation of gene expression at the inner nuclear membrane. LUMA could be a protein responsible for activation of special regions of heterochromatin upon a signal or it could function as an anchor for patches of euchromatin analogously to lamin B receptor`s anchoring of heterochromatin (Minc et al., 1999). More and more evidence accumulates for an active role of INM proteins in gene regulation (see Introduction) but only their function in gene silencing has been investigated so far. LUMA could be the first INM protein that acts as an activator of gene expression. Given that LUMA appeared late in the evolution (it is expressed in flies and vertebrates but not in worms), it seems likely that it has a rather specialized function. Its unusual topology and lack of any homology domains further support this hypothesis. Antibodies against the endogenous protein and studies of LUMA in living cells using GFP fusion proteins are the next steps required to come closer to the function of this protein.

2.3 FUNCTIONAL CHARACTERIZATION OF LAP 2β - THE NATIVE LAP 2β COMPLEXES

In an attempt to characterize the function of LAP 2β, complexes existing at the nuclear envelope were isolated by using different techniques. The aim was to purify complexes containing LAP 2β and to analyze their components. The ultimate goal was to identify interaction partners of LAP 2β.

2.3.1 Solubilization of nuclear envelopes

To isolate complexes of LAP 2β required the development of techniques for solubilizing the NE in a way that does not compromise the stability of such complexes. The usual way of solubilizing INM proteins, a combination of TX-100 and high ionic strength (1M NaCl) is not suitable when the native protein complexes are to be left intact. A detergent was needed that is able to quantitatively solubilize LAP 2β and to not disrupt the protein complexes. Two detergents– n-dodecyl-β-maltoside and Tween 80, were tested with respect to their ability to solubilize LAP 2β from the 'crude' preparation of NE (see Methods, 4.2.7), with or without non-detergent sulfobetaine as an additive. Non-detergent sulfobetaines have been used to improve the efficiency of solubilization of membrane proteins and to isolate nuclear proteins. They are supposed to prevent protein aggregation (Vuillard et al., 1995).
Nuclear envelopes (200 μg of NE protein) were supplemented with detergent and the samples were incubated for 30 min on a shaker at 37 °C. The samples were then centrifuged and the pellets and supernatants applied to SDS-PAGE (see Methods 4.3.2.2). The gels were blotted and the anti LAP 2β antibody was used for immunodetection. Nuclear envelope without addition of detergent was used as control. The results are summarized in fig. 2-22.

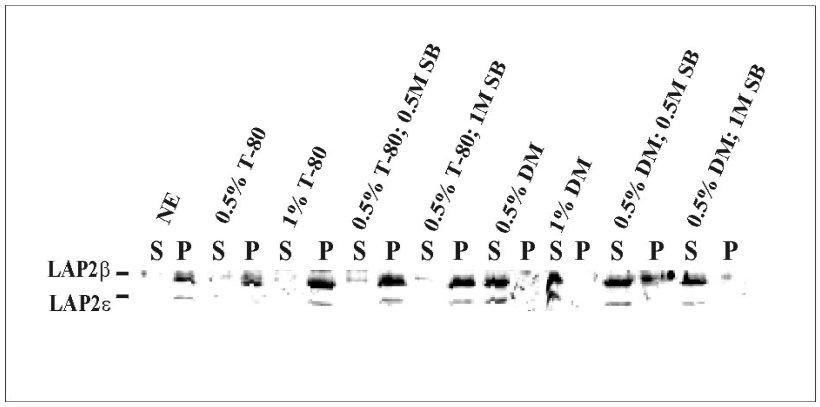

Fig. 2-22 Solubilization of nuclear envelopes, Western blot. Anti-LAP 2β/ε antibody was used for detection. DM: n-dodecyl-β-maltoside, SB: non-detergent sulfobetaine, T-80: Tween 80, S: supernatant, P: pellet, NE: nuclear envelope without detergent.

As can be seen in fig. 2-22, 0.5 % n-dodecyl-β-maltoside is sufficient to quantitatively solubilize LAP 2β from the NE. The addition of non-detergent sulfobetaine or an increased detergent concentration does not improve the solubilization further. Tween 80, with or without non-detergent sulfobetaine, on the other hand, was not capable of solubilizing LAP 2β from the NE. 0.5 % n-dodecyl-β-maltoside was chosen as the detergent for all further experiments.

2.3.2 Gel filtration

2.3.2.1 FPLC

One of the standard methods for the isolation of protein complexes is size exclusion chromatography (gel filtration). Using the solubilization conditions established in the previous experiment, 3 mg of NE proteins were treated with 0.5 % of n-dodecyl-β-maltoside and loaded on an equilibrated Superose 12 FPLC column. The same detergent-containing buffer was used for elution of the proteins and for the calibration of the column.

The calibration was performed using the protein mixture described under Methods. The elution profile is shown in fig. 2–23. The elution volumes of the calibrants were used to estimate the size of LAP 2β-containing protein complexes. The eluted NE proteins were TCA-precipitated, separated on a 10 % SDS-PAGE and checked for their content of LAP 2β. The results are summarized in fig. 2-24.

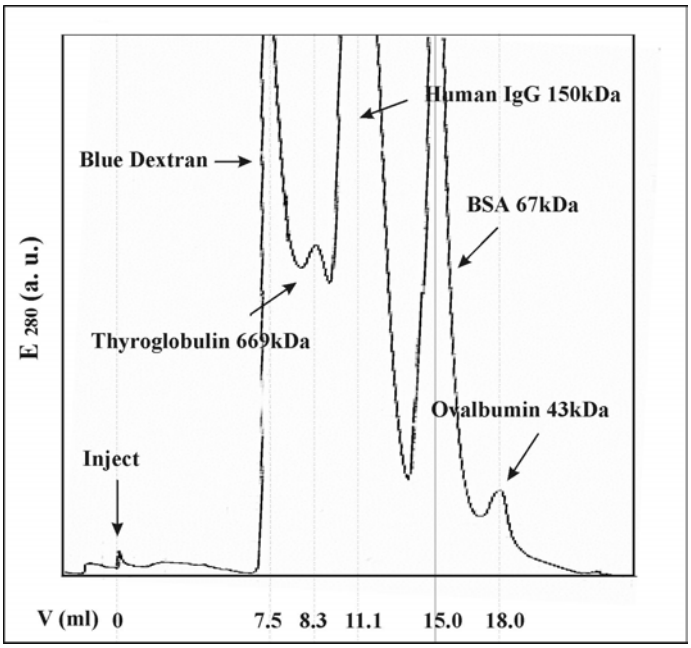

Fig. 2-23 Calibration profile of the Superose 12 FPLC gel filtration column. Void volume: 7.5 ml, the elution volumes of the proteins used for calibration as listed in the figure.

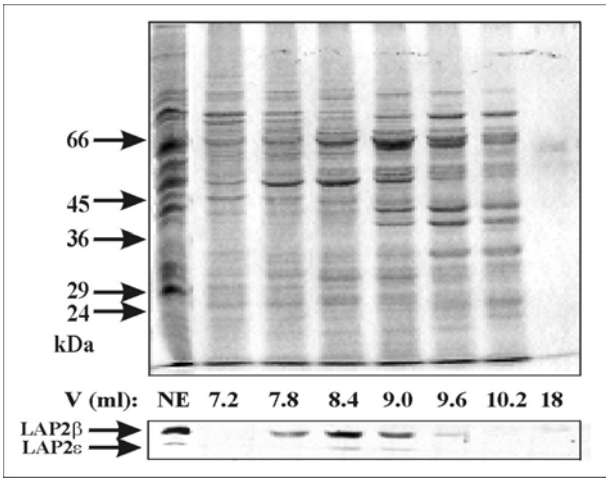

Fig. 2-24 Separation of nuclear envelopes on a Superose 12 gel filtration FPLC column. Nuclear envelopes were solubilized with 0.5 % n-dodecyl-β-maltoside and loaded on the column as described under Methods. The collected fractions were TCA-precipitated and separated on a 10 % SDS-PAGE, then immunoblotted for LAP 2β/ε. Elution volumes of selected fractions are assigned below the lanes.

Most of the LAP 2β/ε can be found in fractions with the elution volumes of 8–9 ml, which corresponds to a molecular weight of ca 500–700kDa. This high molecular weight complex apparently contains LAP 2β and 2ε, since both isoforms eluted in the same fractions. Further

characterization of the complexes did not succeed, mostly due to the complexity of the sample. Therefore, other methods for separation of the complexes were tested.

2.3.2.2 SMART high performance liquid chromatography

Although giving valuable information about the size and, most of all, the existence of high molecular weight LAP 2β/ε complexes at the NE, the Superose 12 column did not efficiently separate the proteins. Therefore, another gel filtration column was tested, the Superdex 200 PC 3.2/30 SMART high performance liquid chromatography gel filtration column, which allows separation of much smaller amounts of protein (300 µg as compared to the 3 mg of the FPLC column). The separation was performed analogous to the FPLC. The column was calibrated, equilibrated and the proteins eluted with the same detergent-containing buffer. The collected fractions were TCA-precipitated and loaded on a 7.5 % SDS-PAGE. To locate LAP 2β, an immunoblot was performed. The calibration profile is shown in fig. 2-25, the immunoblot of selected fractions in fig. 2-26.

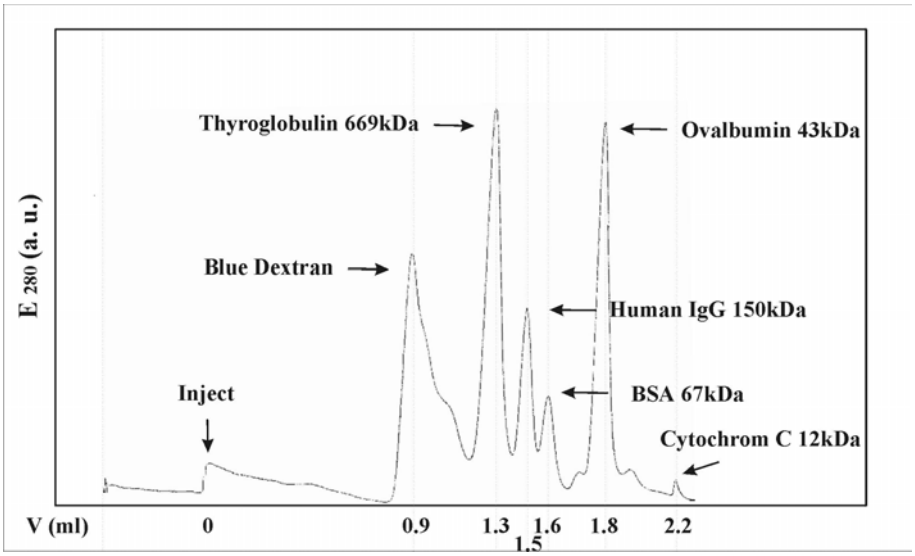

Fig. 2-25 Calibration profile of the Superdex 200 PC 3.2/30 SMART gel filtration column. Void volume: 0.9 ml, the elution volumes of the proteins used for calibration as listed.

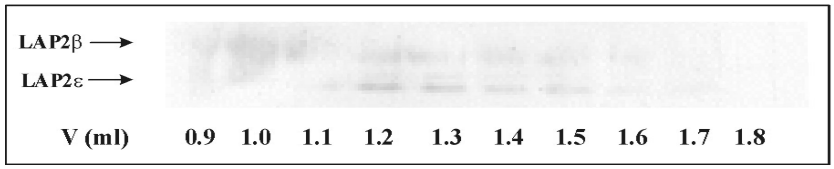

Fig. 2-26 Separation of nuclear envelopes on a Superdex 200 PC 3.2/30 SMART gel filtration column - immunoblot of selected fractions. NE were solubilized with 0.5 % n-dodecyl-β-maltoside and loaded on the column as described under Methods. The collected fractions were TCA-precipitated and separated on a 7.5 % SDS-PAGE, then immunoblotted for LAP 2β/ε. Elution volumes of the shown fractions are given below the lanes.

As in the FPLC experiment, the majority of LAP 2β and LAP 2ε are found in fractions corresponding to very high molecular weights (150–700kDa). This wider distribution of LAP 2β complexes results from the better resolution of the SMART system as can be seen by comparing the calibration runs (fig. 2-25 and 2-23). Nevertheless, also with SMART no satisfactory separation of protein complexes could be achieved. Additionally, the protein amounts were so low, that any attempts to use the eluates for a separation in a second dimension failed.

2.3.3 Glycerol gradient centrifugation

Another common method for the separation of native complexes by size is the glycerol gradient centrifugation. The biggest advantage of this method compared to size exclusion chromatography is that the sample does not have to be filtrated before being loaded on the gradient. That way, no components of the sample are lost during the sample preparation.
Typically, 1 mg of solubilized NE proteins (0.5 % n-dodecyl-β-maltoside) was loaded on a 10–50 % glycerol gradient and centrifuged over night as described under Methods. The collected fractions were analyzed by SDS-PAGE and Western blot to locate LAP 2β (fig. 2-27). Cross-linked GluDH was treated like the solubilized NE and used as a molecular weight size marker (fig. 2-28).

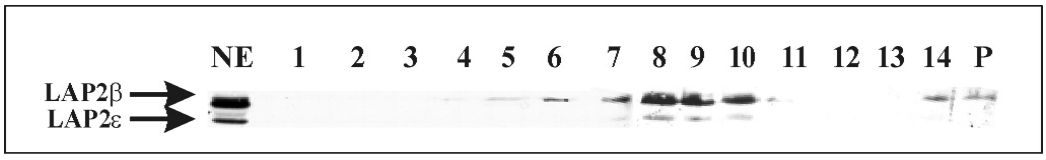

Fig. 2-27 Glycerol gradient centrifugation of solubilized nuclear envelopes. Western blot of the collected fractions. Fraction 1: top, fraction 15 is the pellet. The anti-LAP 2β/ε antibody was used for detection.

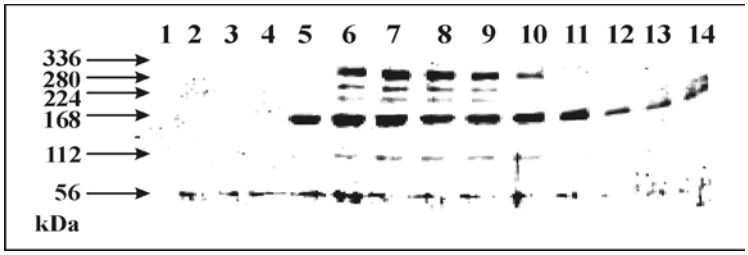

Fig. 2-28 Glycerol gradient centrifugation of cross–linked GluDH. Western blot of the collected fractions. Fraction 1: top, fraction 14: bottom. The anti-GluDH antibody was used for detection.

As can be seen in fig. 2-27, most of LAP 2β and 2ε can be found in fractions 8–10. When compared to the calibration gradient (fig. 2-28), these fractions seem to contain complexes of molecular weights equal or larger than 336kDa. Some LAP 2β also ended up in the pellet, indicating the existence of even larger complexes. The largest complexes are void of LAP 2ε. One has to keep in mind, however, that the size information is not very reliable. GluDH apparently is not the perfect choice for a marker, since it appears in a wide range of the gradient. Still, the results for glycerol gradient centrifugation are consistent with those from gel filtration, but here a second separation method would also be necessary for further characterization of the complexes. An attempt to cross-link the protein complexes in the interesting fractions did not succeed, probably because of the high amount of glycerol in the sample. Any other method, like size exclusion chromatography or blue native electrophoresis, would fail for the same reasons.

2.3.4 Blue Native Gel Electrophoresis

As a last attempt to analyse the native complexes of LAP 2β, two-dimensional blue native gel electrophoresis was used. By this method, protein complexes are also separated by size, but in

contrast to the other methods used, having access to suitable antibodies, it can be seen directly if the proteins are members of the same complex.

Typically, 200 µg of nuclear envelope protein (treated as described in Methods) were loaded on a 4-16 % Blue Native Gel. After completion of the run, the gel was blotted and the blot was sequentially probed with appropriate antibodies. In parallel, an identical gel was used for the second dimension, by cutting out the whole lane and applying it to the SDS-PAGE, as described in Methods. The second dimension gel was also blotted and the blot was sequentially probed with the same antibodies. The results are summarized in fig. 2-29.

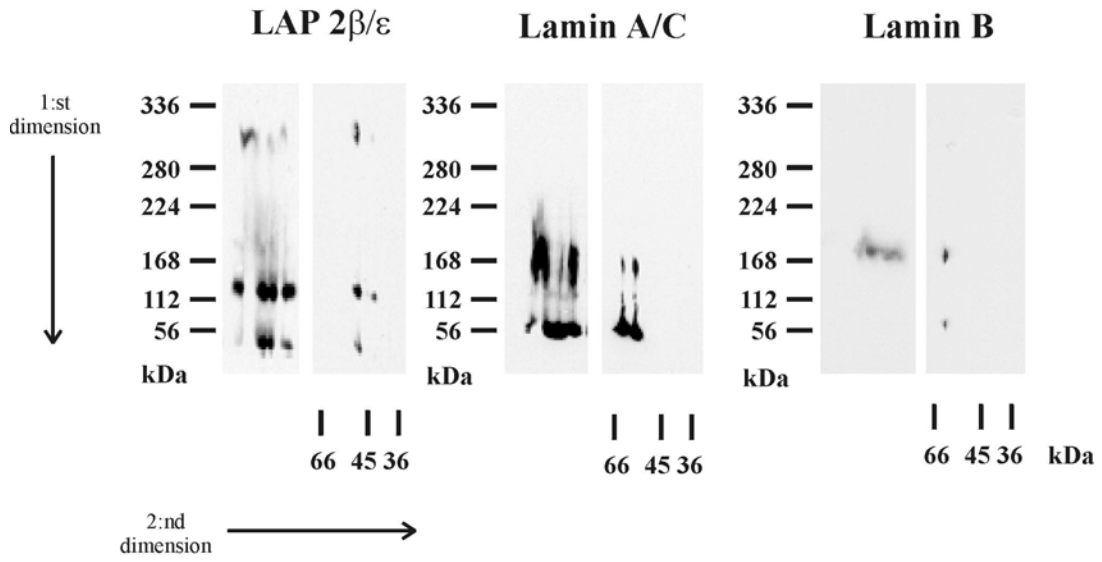

Fig. 2-29 Blue Native Gel Electrophoresis of solubilized nuclear envelopes. Western blot of the pairwise first (left) and second (right) dimension. The three images correspond to the same lane which was sequentially probed with different antibodies, anti-LAP 2β/ε, anti-lamin A/C and anti-lamin B. Cross-linked GluDH was used as a size marker for the first dimension. LAP 2β and LAP 2ε can be found in high molecular weight complexes which do not contain lamina.

Complexes containing LAP 2β/ε could be detected at approximate molecular weights of 120 and 300kDa. Neither of these complexes contains lamin A/C or B. The lighter complex contains LAP 2β and 2ε and other compounds which provide additional 20 kDa. It is tempting to speculate, that this other compound is BAF. BAF has a molecular weight of 10 kDa and is known to interact with LAP 2β and coordinate its binding to DNA (Furukawa K., 1999). Since an antibody against BAF was not available, its presence in the complex could not be tested.

The ~300kDa complex would be most interesting for further investigation. The number of available antibodies against nuclear envelope proteins is very limited, therefore further characterization of the complexes would have to be designed as a proteomic analysis. Every spot from a second dimension gel should be identified, all candidate interacting proteins should then be produced recombinantly and tested for their binding to LAP 2β *in vitro* as well as their colocalization at the nuclear envelope.